Rb deficiency during *Drosophila* eye development deregulates EMC, causing defects in the development of photoreceptors and cone cells

Milena K. Popova[1], Wei He[1], Michael Korenjak[2], Nicholas J. Dyson[2] and Nam-Sung Moon[1,*]

[1]Department of Biology, Developmental Biology Research Initiative, McGill University, Montreal, Quebec H3A 1B1, Canada
[2]Massachusetts General Hospital Cancer Research Center and Harvard Medical School, Charlestown, MA 02129, USA
*Author for correspondence (nam.moon@mcgill.ca)

Journal of Cell Science

Summary

Retinoblastoma tumor suppressor protein (pRb) regulates various biological processes during development and tumorigenesis. Although the molecular mechanism by which pRb controls cell cycle progression is well characterized, how pRb promotes cell-type specification and differentiation is less understood. Here, we report that Extra Macrochaetae (EMC), the *Drosophila* homolog of inhibitor of DNA binding/differentiation (ID), is an important protein contributing to the developmental defects caused by Rb deficiency. An *emc* allele was identified from a genetic screen designed to identify factors that, when overexpressed, cooperate with mutations in *rbf1*, which encodes one of the two Rb proteins found in *Drosophila*. EMC overexpression in an *rbf1* hypomorphic mutant background induces cone cell and photoreceptor defects but has negligible effects in the wild-type background. Interestingly, a substantial fraction of the *rbf1*-null ommatidia normally exhibit similar cone cell and photoreceptor defects in the absence of ectopic EMC expression. Detailed EMC expression analyses revealed that RBF1 suppresses expression of both endogenous and ectopic EMC protein in photoreceptors, thus explaining the synergistic effect between EMC overexpression and *rbf1* mutations, and the developmental defect observed in *rbf1*-null ommatidia. Our findings demonstrate that ID family proteins are an evolutionarily conserved determinant of Rb-deficient cells, and play an important role during development.

Key words: *rbf1*, Retinoblastoma, *emc*, ID, Development

Introduction

Retinoblastoma tumor suppressor protein (pRb) is an evolutionarily conserved protein whose activity controls various biological processes. The best-characterized function of pRb is to regulate cell cycle progression (Dyson, 1998). Inactivation of Rb family proteins in multicellular organisms, such as insects and mammals, often leads to additional rounds of cellular division during development (van den Heuvel and Dyson, 2008). One of the key molecular targets of Rb family proteins is the E2F transcription factor that regulates the expression of genes that are involved in DNA synthesis and cell cycle progression. In quiescent cells, Rb family proteins physically bind to E2F and act as transcriptional co-repressors. In cycling cells, Rb family proteins are regulated by cyclin-dependent kinases, thus coupling the expression of E2F target genes to different phases of the cell cycle. As a result, in most cancer cells where Rb family proteins are functionally inactive, expression of E2F target genes is no longer regulated in a cell cycle-dependent manner (Sherr, 1996). Importantly, in addition to E2F, pRb tumor suppressor proteins physically interact with and regulate the activities of other cell cycle regulators such as S-phase kinase-associated protein 2 (Skp2) and anaphase-promoting complex (APC) (Binne et al., 2007; Ji et al., 2004). A recent study demonstrated that, like E2F, Skp2 is required for the tumorigenesis in *pRb* heterozygous mice (Wang et al., 2010), demonstrating that the tumors generated by pRb deficiency are the result of deregulation of multiple factors such as E2F and Skp2.

In addition to the role of pRb during cell cycle progression, evidence from mouse studies indicates that pRb also participates in cell-type specification and differentiation processes. Various developmental defects in the nervous, muscular and hematopoietic systems have been identified in *pRb* knockout mice (Lipinski and Jacks, 1999). More recently, pRb was shown to regulate the cell-fate choice of mesenchymal progenitors during development, and to influence the identity of cell lineages susceptible to tumorigenesis (Calo et al., 2010). At the molecular level, pRb has been shown to physically associate with transcription factors that are directly involved in cell-fate specification. For example, pRb physically binds to MyoD to promote expression of muscle-specific genes and to Runx2 to promote osteogenic differentiation (Gu et al., 1993; Thomas et al., 2001). Despite these findings, the exact molecular mechanism by which the inactivation of pRb interferes with cell-type specification and differentiation processes remains unclear.

One factor that was shown to have both physical and genetic interactions with pRb is inhibitor of DNA binding/differentiation 2 (ID2). ID family proteins contain helix-loop-helix (HLH) domains for protein–protein interactions but lack a DNA binding domain. Therefore, they function as dominant-negative proteins to other transcription factors with a HLH domain (Lasorella et al., 2001). Genetic studies in mice demonstrated that the *Id2* mutation suppresses numerous developmental defects observed in *pRb* knockout mice (Iavarone et al., 2004; Lasorella et al.,

2000). Moreover, ID2 ablation was shown to delay tumor onset and decrease the number and size of early focal lesions observed in *pRb* heterozygous mice (Lasorella et al., 2005). These findings support the idea that pRb normally limits the activity of ID2 during development, and that deregulated ID2 activity contributes to the tumorigenesis of pRb-deficient cells. A possible molecular explanation for these genetic interactions was previously provided by the observation that the hypophosphorylated form of pRb physically binds to ID2 (Iavarone et al., 1994; Lasorella et al., 1996), suggesting that pRb might prevent ID2 from interacting with other transcription factors. Currently, it is not known whether the genetic interaction between *pRb* and *Id2* is caused by the physical interaction between their products.

Drosophila melanogaster serves as a useful model system to investigate the in vivo function of a gene in a developmental context. *Drosophila* encodes two Rb family proteins, RBF1 and RBF2 (van den Heuvel and Dyson, 2008). Although the effect of *rbf* mutations on cell cycle progression and survival are well characterized, their role in differentiation is less understood. Genome-wide transcriptome analysis clearly demonstrated that RBF1 and RBF2 directly bind to and regulate expression of many genes that potentially have consequences on differentiation (Dimova et al., 2003; Stevaux et al., 2005). However, no obvious cell cycle- or cell death-independent developmental defects have been associated with *rbf* single or double mutant flies. A recent study demonstrated that *rbf1* mutations can cooperate with *warts* mutations to interfere with photoreceptor differentiation (Nicolay et al., 2010). Moreover, a genetic screen designed to discover mutations that can cooperate with *rbf1* mutations identified Rhinoceros as a protein that cooperates with RBF1 to promote R8 photoreceptor development (Steele et al., 2009). Perhaps, the *rbf1* mutation itself might not be sufficient to cause a visible phenotype, but it might cause important changes that render cells more susceptible to other genetic alterations.

We sought to identify factors that can specifically cooperate with *rbf1* mutations. We reasoned that the identification of such factors could help us to determine pathways deregulated by the loss of Rb family proteins, and to understand how Rb-deficient cells respond to additional genetic changes. This idea led us to conduct a mis-expression genetic screen in *Drosophila* to identify factors that, when overexpressed, induce an eye phenotype specifically in an *rbf1* mutant background. An Exelixis stock that can induce overexpression of Extra Macrochaetae (EMC) was identified from this genetic screen. Interestingly, EMC is the *Drosophila* homolog of ID family proteins, suggesting that the relationship between Rb and ID family proteins is evolutionarily conserved. Overexpression of EMC in the eye of a hypomorphic *rbf1* allele, *rbf1^{120a}*, induced formation of ommatidia with abnormal numbers of cone cells and photoreceptors. Interestingly, similar developmental defects were observed in a substantial fraction of *rbf1*-null mutant ommatidia without overexpressing EMC. The molecular aspect of the ommatidial defects was elucidated, at least in part, by the observation that RBF1 post-transcriptionally regulates the expression of both endogenous and ectopic EMC proteins. Our findings provide evidence suggesting that ID family proteins are an important determinant of developmental defects caused by Rb deficiency in both flies and mammals.

Results

In an attempt to identify factors that can cooperate with *rbf1* mutations, a genetic screen that utilizes a viable hypomorphic allele of *rbf1*, *rbf1^{120a}* was designed. Although cell cycle and cell death defects have been found in *rbf1^{120a}* mutant larvae, the adult eyes of *rbf1^{120a}* appear relatively normal (Fig. 1B) (Du and Dyson, 1999; Moon et al., 2006). We reasoned that *rbf1^{120a}* represents a hypersensitized genetic background where factors that can cooperate with *rbf1* mutations could be identified. This led us to establish tester stocks where any *UAS*-transgenes can be expressed in wild-type and *rbf1^{120a}* backgrounds in an eye-specific manner (see Materials and Methods). The Exelixis stock collection at Harvard Medical School was used as the source of *UAS*-transgenes. A subset of Exelixis collection was generated by inserting *XP* vectors at random sites in the *Drosophila* genome (Thibault et al., 2004). An *XP* vector carries two UAS enhancer elements that can be activated by Gal4 to bidirectionally overexpress genes neighboring the insertion site. Because one of the two UAS elements in the vector is flanked by Flip-recombinase target (FRT) sequences, and our tester stocks express eye-specific Flip-recombinase (see Materials and Methods), we presumed that the gene primarily mis-expressed in our screen is downstream of the UAS element not flanked by FRT sequences. After crossing our tester stocks to the *XP* collection, we identified stocks that produced *rbf1^{120a}* mutant eye-specific phenotypes (Fig. 1A). We screened approximately 3500 stocks and identified 11 that had a reproducible effect in the *rbf1^{120a}* mutant background. Although to a lesser extent, most stocks identified from the screen had a small effect in the wild-type background. Among the 11 stocks identified, *d09015* produced the most specific effect in the *rbf1^{120a}* mutant eyes (Fig. 1B). *d09015* in the *rbf1^{120a}* mutant background induced roughness and reduction in overall size of the eye. We also noted that *d09015* in both wild-type and the *rbf1^{120a}* backgrounds produced eyes in which bristles were missing. Immunostaining against Cleaved Caspase 3 (C3) revealed that the level of cell death normally observed in *rbf1^{120a}* eye discs was largely unaffected by *d09015*, indicating that the specific eye phenotype induced by *d09015* in the *rbf1^{120a}* background was not caused by an excessive amount of cell death (Fig. 1C). This result indicates that *d09015* contains an *XP* insertion next to a gene that, when overexpressed, cooperates with *rbf1* mutations to interfere with *Drosophila* eye development. We decided to further characterize *d09015* because of the specificity of its effect in the *rbf1^{120a}* background.

The insertion sites of the Exelixis collection have been sequenced (Thibault et al., 2004). According to the information provided, *d09015* has an *XP* insertion on the second chromosome, upstream of a micro-RNA cluster mir-310 to mir-313. However, we quickly realized that *d09015* carries a transgene that segregates with the third chromosome. This led us to sequence the integration site of the *XP* vector. The sequencing result revealed that *d09015* carries an *XP* insertion 72 bp upstream of *emc*, a helix-loop-helix (HLH) motif-containing gene (Fig. 2A). We tested whether mis-expression of *emc* is capable of recapitulating the eye phenotype generated by *d09015* by taking advantage of a previously characterized *UAS-emc* transgene (Adam and Montell, 2004). We used the same tester stocks to drive expression of *emc* in the control and *rbf1^{120a}* eyes. As shown in Fig. 2B, similarly to *d09015*, overexpression of *emc* produced an eye phenotype in an
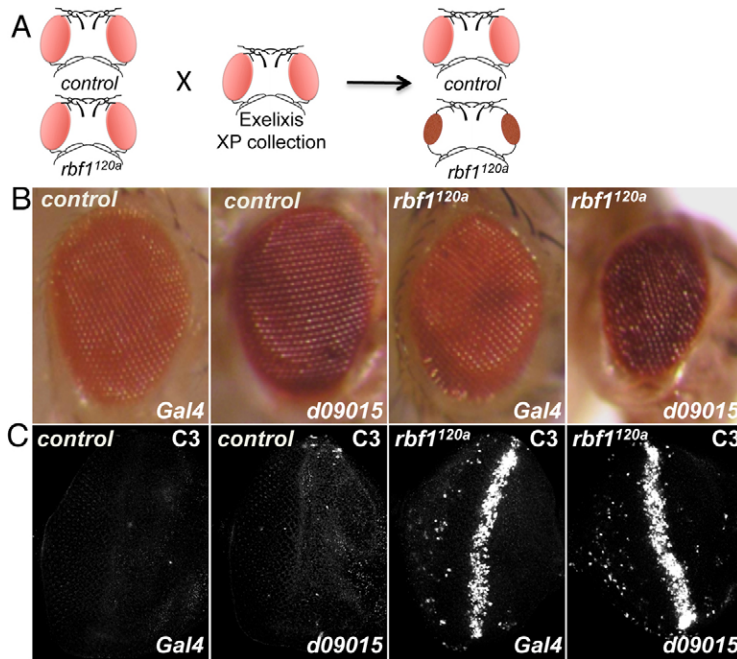
Fig. 1. The *d09015* Exelixis allele differently affects the eye development of wild-type and *rbf1^{120a}* mutant flies. (A) Cartoon illustrating the genetic screen. An eye-specific Gal4 driver, *ey-FLP; Act5C>CD2>Gal4,* was introduced in wild-type (control) and *rbf1^{120a}* hypomorphic (*rbf1^{120a}*) mutant backgrounds. These tester flies were crossed to the Exelixis *XP* collection, and alleles that produced an eye phenotype specifically in the *rbf1* mutant background were identified. (B) Adult male eyes of the tester alleles and of the tester alleles crossed to the *d09015* allele. (C) Eye imaginal discs (corresponding to the flies in B) were stained with an anti-C3 to visualize dying cells.

rbf1^{120a}-specific manner. Moreover, similarly to *d09015, emc* overexpression produced adult eyes with no bristles in both control and *rbf1^{120a}* backgrounds. Because *d09015* is homozygous lethal, we performed a genetic complementation test to determine whether *d09015* is an *emc* allele. We crossed *d09015* flies to a known *emc* allele, *emc¹*, that carries a point mutation in the HLH domain. The *d09015/emc¹* trans-heterozygous flies displayed the extra macrochaetae phenotype (Fig. 2C), indicating that *d09015* is allelic to *emc*. These results indicate that the effect of *d09015* on *rbf1^{120a}* mutant eyes is the result of *emc* overexpression.

A recent study demonstrated that *emc* is required for R7 photoreceptor and cone cell development (Bhattacharya and Baker, 2009). This prompted us to investigate the cellular defect caused by *d09015* in *rbf1^{120a}* eyes. Pupal eye discs 42 hours after puparium formation (APF) were co-immunostained with anti-ELAV and anti-Cut antibodies to visualize photoreceptors and cone cells, respectively (Fig. 3A). We could not detect any obvious neuronal or cone cell defects in the control background in the presence or absence of *d09015*. ELAV and Cut staining patterns were also relatively normal in the *rbf1^{120a}* background, although we occasionally detected a few ommatidia with an abnormal number of cone cells (data not shown). By contrast, in the *rbf1^{120a}* background where *emc* was overexpressed through *d09015*, we frequently detected ommatidia with less than four cone cells per cluster (Fig. 3A, yellow arrows). Moreover, we also noticed that the ommatidia associated with cone cell defects also displayed an irregular pattern of ELAV staining. To better examine the ELAV staining pattern, pupal eye discs were co-immunostained with anti-ELAV and anti-Chaoptin antibodies (Fig. 3B). Chaoptin is specifically expressed in photoreceptors and localizes to the plasma membrane (Reinke et al., 1988). The co-immunostaining for ELAV and Chaoptin allowed us to count the number of photoreceptors per ommatidium. Normally, each ommatidium contains eight ELAV-positive photoreceptors. As shown in Fig. 3B, ommatidia in *rbf1^{120a}* mutant eyes expressing *emc* frequently contained less than eight photoreceptors.

Importantly, the same defects were observed when the *UAS-emc* transgene was used to overexpress *emc* in the *rbf1^{120a}* mutant background (data not shown). To understand the nature of the photoreceptor defect, third-instar eye imaginal discs were immunostained for cell-type specific proteins: Senseless for R8, Rough for R2 and R5, and Lozenge (Lz) for R1, R6 and R7 photoreceptors. Photoreceptors are specified in sequence during *Drosophila* eye development: R8 is the first to be specified, followed by R2/R5, R3/4, R1/6, and R7 is the last photoreceptor to be determined. The Senseless expression pattern was not altered by EMC overexpression either in wild-type or *rbf1^{120a}* mutant eye discs (supplementary material Fig. S1A). The Rough expression pattern was disrupted in *rbf1^{120a}* mutant eye discs by overexpressing EMC; however, the majority of ommatidia clusters contained two Rough-expressing cells, suggesting that R2 and R5 photoreceptor specification was not greatly affected (supplementary material Fig. S1A). Interestingly, Lz expression was significantly delayed in *rbf1^{120a}* mutant eye discs overexpressing EMC, and was absent in several photoreceptor clusters in the posterior region of the eye disc (Fig. 3C). Overall, EMC overexpression can interfere with a subset of photoreceptors and cone cell development when the function of RBF1 is compromised.

In mammals, there are four *emc* homologs, *Id1–Id4*. As mentioned in the Introduction, physical association between pRb and ID2 has been previously reported (Iavarone et al., 1994). Therefore, we tested whether RBF1 could also physically interact with EMC by performing a co-immunoprecipitation assay in S2 cells. However, we could not detect any appreciable protein–protein interaction between the two proteins. Similar results were obtained with protein extracts prepared from *Drosophila* adult heads (supplementary material Fig. S2 and see Discussion). Because RBF1 is a repressor of transcription, we next asked whether expression levels or patterns of EMC staining are altered in *rbf1* mutant cells. Immunostaining of larval eye imaginal discs containing *rbf1*-null, *rbf1⁴¹⁴*, mutant clones revealed that the intensity of EMC staining was stronger in *rbf1* mutant cells,
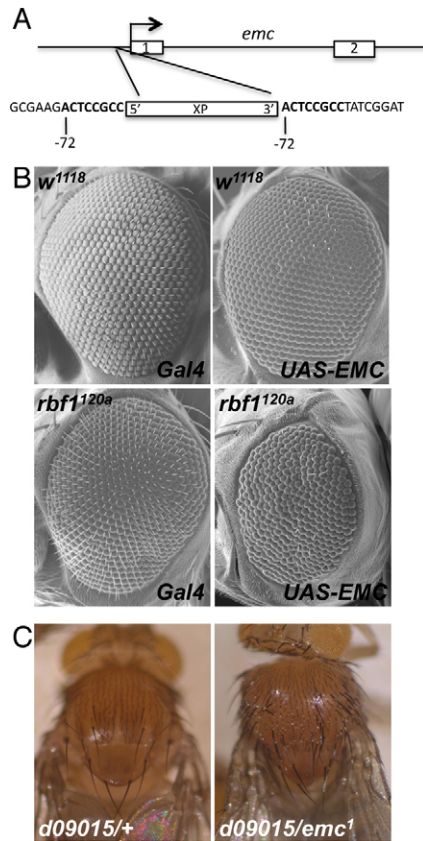
Fig. 2. The *d09015* allele is an *emc* allele that contains an *XP* vector insertion 72 bp upstream of the *emc* transcription start site.
(**A**) Representation depicting the *XP* vector insertion in the *d09015* allele. Sequencing the genomic DNA of the *d09015* allele revealed that the *XP* vector is inserted 72 bp upstream of the *emc* transcription start site. (**B**) SEM images of *Drosophila* adult male eyes of the tester alleles and of the tester alleles crossed to a previously published *UAS-emc* transgenic allele. Note that *UAS-emc* is capable of inducing an eye phenotype specifically in the *rbf1^{120a}* background. (**C**) Dorsal views of a *d09015* heterozygous adult fly and a *d09015/emc^1* trans-heterozygous adult fly. Note the extra bristles in the trans-heterozygous *d09015/emc^1* adult fly.

particularly in the posterior region of the eye disc (Fig. 4A). The pattern of EMC staining led us to suspect that EMC is specifically deregulated in the differentiating photoreceptors. Co-immunostaining of eye discs with anti-EMC and anti-ELAV antibodies confirmed that the level of EMC is increased in the *rbf1^{Δ14}* mutant photoreceptors (Fig. 4B).

Deregulated EMC expression in the *rbf1* mutant clones prompted us to look closely at the ommatidial development in *rbf1^{Δ14}* mutant clones. Because the overexpression of EMC can cooperate with hypomorphic *rbf1* mutations (Fig. 3), we asked whether a similar developmental defect could be observed in an *rbf1*-null background where EMC expression is normally deregulated. In fact, cone cell defects for another *rbf1*-null mutant allele have been recently described (Steele et al., 2009). Immunostainings for Cut, a cone cell marker, confirmed that cone cell defects were present in *rbf1^{Δ14}* mutant clones (Fig. 5A). More importantly, similar to observations with EMC overexpression in the *rbf1^{120a}* background, we frequently detected irregular patterns of ELAV staining in *rbf1^{Δ14}* ommatidia with cone cell abnormalities (Fig. 5A, arrows). In

addition, Lz expression was also delayed in *rbf1^{Δ14}* mutant clones at the third-instar larval stage (supplementary material Fig. S1B). To be able to clearly count the number of photoreceptors per ommatidium, immunostaining with anti-ELAV and anti-Chaoptin antibodies was carried out (Fig. 5B). A number of *rbf1^{Δ14}* ommatidia appeared to contain an abnormal number of photoreceptors. To determine the frequency of this phenotype, we counted the number of photoreceptors within each ommatidium. For this analysis, we only examined ommatidia that were entirely composed of either *rbf1^{Δ14}* or wild-type cells. As shown in Fig. 5C, 99% of control ommatidia contained eight photoreceptors per cluster ($n=599$), as expected. As for those ommatidia entirely composed of *rbf1^{Δ14}* photoreceptors, more than one third of ommatidia contained less than eight photoreceptors per ommatidium ($n=641$), indicating that RBF1 is required for proper formation of the ommatidial cluster.

Considering the role of *rbf1* in survival, it is possible that the decrease in the number of photoreceptors is due to an increased level of cell death. To examine this possibility, we repeated the clonal analysis with eye discs expressing a baculoviral cell death inhibitor, p35. During *Drosophila* eye development, a wave of programmed cell death at the pupal stage eliminates the surplus of cells that are not incorporated into ommatidia. Any excess of cells that survive this process end up occupying interommatidial space, and can be visualized by anti-Disc Large (Dlg) immunostaining. Normally, there should be only one tertiary pigment cell occupying each side of hexagonal ommatidia. As shown in Fig. 6A, we could detect extra interommatidial cells in the eye discs expressing p35, confirming that programmed cell death was indeed inhibited (Fig. 6A). This was particularly true in *rbf1^{Δ14}* clones where more than one row of interommatidial cells could be observed. Co-immunostaining with anti-ELAV and anti-Cut antibodies revealed that the ommatidial defect was still present, despite cell death being suppressed (Fig. 6B). In fact, we even found some ommatidia with the correct number of cone cells displaying an abnormal pattern of ELAV staining, suggesting that p35 might actually enhance the phenotype (Fig. 6B, asterisk). We therefore performed immunostaining with an anti-Chaoptin antibody to quantify the photoreceptor defects (Fig. 6C,D). As shown in Fig. 6D, more than 80% of *rbf1^{Δ14}* ommatidia contained less than eight photoreceptors when cell death was inhibited ($n=451$). In addition, ommatidia with less than seven photoreceptors appeared to be more frequent than *rbf1^{Δ14}* mutant ommatidia without p35 expression. This result demonstrates that the defects observed in *rbf1^{Δ14}* ommatidia are not likely to be the result of an increased level of cell death.

To determine whether RBF1 controls EMC expression by regulating *emc* transcription, we took advantage of the *emc^{P5c}* allele where β-galactosidase (β-Gal) is expressed under the control of the endogenous *emc* promoter. We generated *rbf1^{Δ14}* mutant clones in eye discs that carried a copy of the *emc^{P5c}* chromosome (Fig. 7). Immunostaining for β-Gal and EMC revealed that the promoter activity of *emc* was reduced in the same *rbf1^{Δ14}* mutant clone where EMC protein expression was increased. This result suggests that, if anything, RBF1 promotes the transcription of *emc*, and that the mechanism by which RBF1 suppresses EMC expression is post-transcriptional.

We also generated a GFP-tagged EMC construct (GFP–EMC) to monitor the expression of ectopically expressed EMC protein. Importantly, GFP–EMC overexpression in the control and *rbf1^{120a}* tester stocks recapitulated the same adult eye
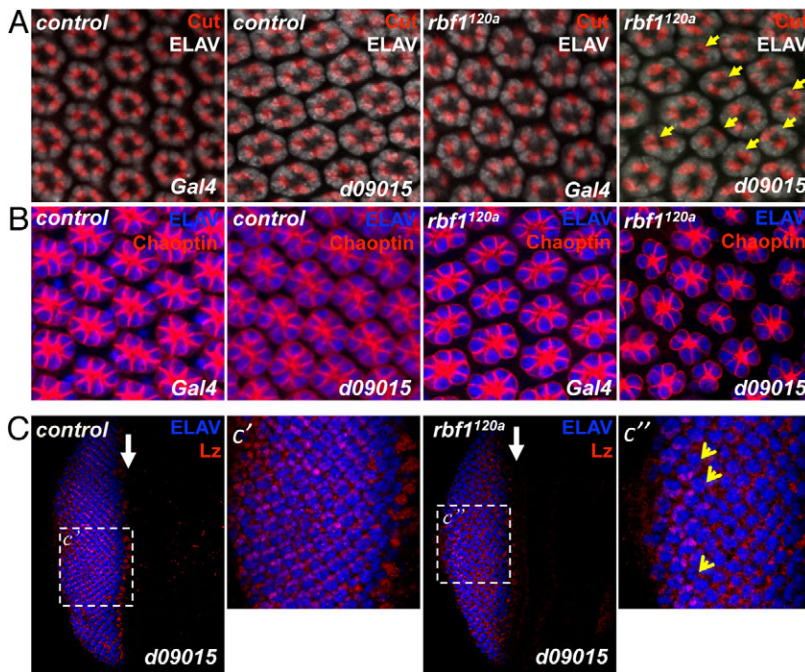
Fig. 3. The *d09015* allele in the *rbf1^120a* background induces cone cell and photoreceptor defects. (**A**) Pupal eye discs (42 hours APF) of control and *rbf1^120a* tester flies by themselves or crossed with the *d09015* allele were stained with anti-ELAV (white) and anti-Cut (red) antibodies. ELAV is a marker for photoreceptors and Cut is a marker for cone cells. Note that the abnormalities in the cone cell staining pattern in the *rbf1^120a* mutant flies that overexpress EMC (*d09015*) are often associated with irregular ELAV staining patterns (yellow arrows). The merged image was generated by overlaying the anti-ELAV image with the anti-Cut image taken at a different focal plane in the same field of vision. (**B**) Pupal eye discs (42 hours APF) of indicated genotypes were stained with anti-ELAV (blue) and anti-Chaoptin (red) antibodies. Chaoptin is a glycoprotein specifically expressed in photoreceptors and localized to the membrane. Note the irregular pattern and abnormal number of photoreceptors in *rbf1^120a* tester flies crossed to *d09015*. (**C**) Third-instar eye discs of indicated genotypes were stained with anti-ELAV and anti-Lz antibodies. Note that Lz expression is delayed in *rbf1^120a* eye discs overexpressing EMC and is missing in several photoreceptor clusters at the posterior region (yellow arrowheads). The position of the MF is marked by white arrows.

phenotype induced by the untagged EMC, indicating that the GFP tag does not interfere with EMC function (data not shown). We first expressed GFP–EMC in the wild-type background using the same Gal4 driver used in the genetic screen. Confocal images of the apical plane of the eye disc immunostained with anti-ELAV antibody revealed that GFP–EMC expression was suppressed in differentiating photoreceptors (Fig. 8A). We observed that the GFP signal was weaker in ELAV-expressing cells than in cells anterior to the morphogenetic furrow (MF) and cells between the ELAV-positive clusters. We did, however, occasionally detect some ELAV-positive cells that expressed a relatively high level of GFP–EMC (Fig. 8A, yellow arrows). This reduction in GFP–EMC expression in photoreceptors was not due to the differential activity of the Gal4 driver because the same driver can drive expression of GFP alone in ELAV-positive cells (supplementary material Fig. S3). In fact, the same driver preferentially expresses GFP in ELAV-positive cells. We then

expressed GFP–EMC in eye discs containing *rbf1^Δ14* mutant clones to ask whether RBF1 participates in suppression of GFP–EMC expression. We performed the experiment at 18˚C to minimize the expression level of GFP–EMC, hoping to limit the overall activity of ectopic EMC. However, we still observed irregularities in the pattern of ELAV staining in the *rbf1^Δ14* clones (Fig. 8B). Considering the phenotype observed in the *rbf1^120a* background, this observation was not unexpected (Fig. 3). On the other hand, the ELAV staining pattern in the wild-type clones was normal, demonstrating again the synergistic effect of EMC overexpression and *rbf1* mutation. Importantly, we could more frequently detect ommatidia that contained one or more ELAV-positive cells expressing a high level of GFP–EMC in *rbf1^Δ14* clones compared with the neighboring control clones (Fig. 8B, yellow arrows). Although we did not quantitatively measure the intensity of the GFP signal, we counted the number of ommatidia that contained one or more ELAV-positive cells
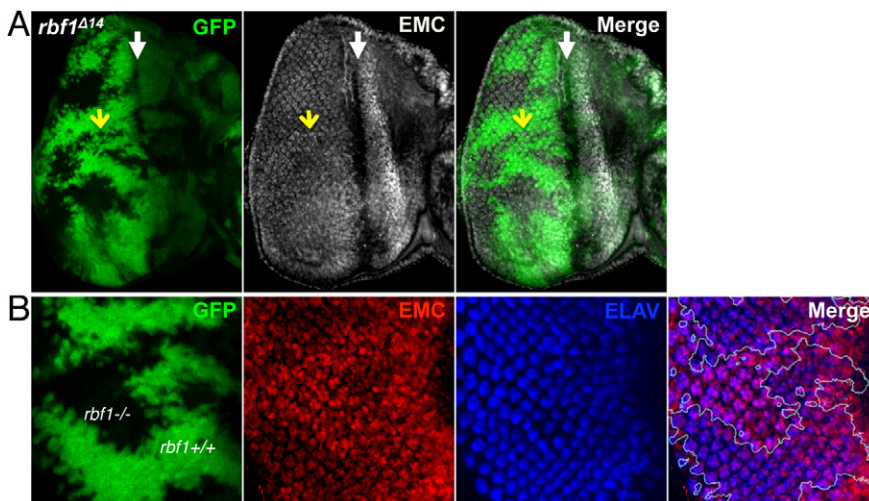

Fig. 4. Expression of endogenous EMC protein is increased in *rbf1* mutant photoreceptors. Mosaic clones of an *rbf1*-null allele, *rbf1^Δ14*, were generated in third-instar larval eye discs using *eyFLP*. The *rbf1^Δ14* mutant clones are marked by the lack of GFP signal. (**A**) Anti-EMC antibody (red) was used to compare the expression pattern of EMC in the wild-type and *rbf1* mutant clones. The position of the MF is marked by white arrows. The yellow arrow indicates a small *rbf1^Δ14* clone where EMC expression was increased. (**B**) Posterior region of an eye disc containing *rbf1^Δ14* mutant clones. The disc was co-stained with anti-EMC (red) and anti-ELAV (blue) antibodies. Note the overlap between EMC and ELAV signals in the *rbf1^Δ14* mutant clones, indicating that EMC expression was deregulated in the *rbf1^Δ14* mutant photoreceptors.
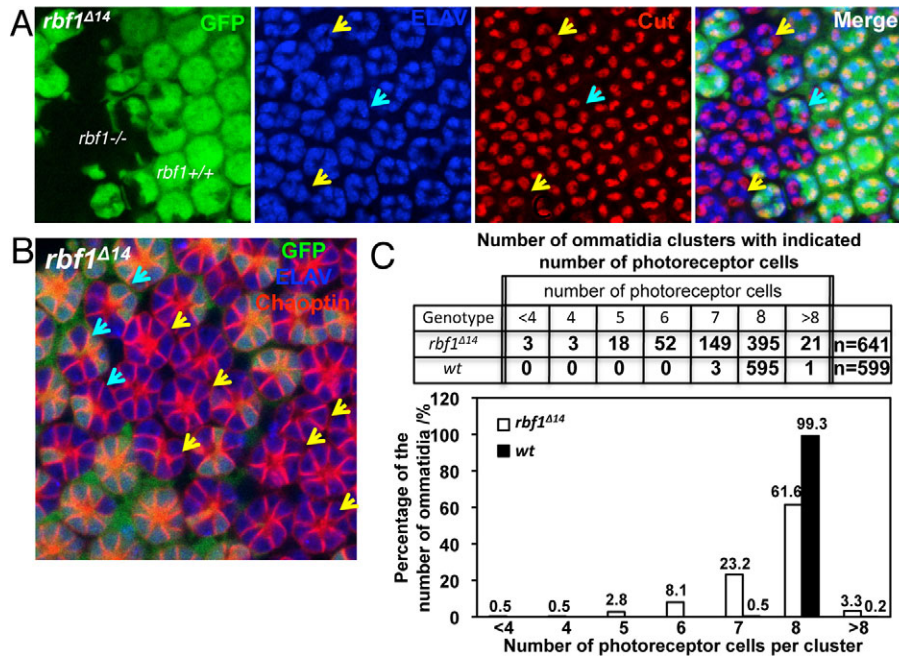
Fig. 5. A subset of $rbf1^{\Delta14}$ mutant ommatidia contains abnormal numbers of cone cells and photoreceptors. (**A**) Mosaic clones of $rbf1^{\Delta14}$ were generated using *eyFLP*. The $rbf1^{\Delta14}$ mutant clones are marked by the lack of GFP signal. Pupal eye discs (42 hours APF) were immunostained with anti-ELAV (blue) and anti-Cut (red) antibodies. The merged image was generated by overlaying anti-ELAV with anti-Cut images taken at different focal planes in the same field of vision. Arrows point out ommatidia clusters with abnormal numbers of cone cells and irregular patterns of ELAV staining (yellow arrows, *rbf1* mutant ommatidia; cyan arrows, mosaic ommatidia composed of *rbf1* mutant and wild-type cells). (**B**) To be able to count the number of photoreceptors, the pupal eye discs described in A were immunostained with anti-ELAV (blue) and anti-Chaoptin (red) antibodies. The $rbf1^{\Delta14}$ mutant clones are marked by the absence of GFP.
(**C**) Approximately 1200 control and $rbf1^{\Delta14}$ mutant ommatidia were analyzed to determine the number of photoreceptors per ommatidium. The table indicates the raw numbers of ommatidia clusters with indicated number of photoreceptor cells. The bar graph shows the percentages of ommatidia (*y*-axis) with the number of photoreceptors indicated on the *x*-axis. In the control background, 99% of the ommatidial clusters contained eight photoreceptors, as expected. However, in the $rbf1^{\Delta14}$ null background, only 62% of the clusters contained eight photoreceptors.

that displayed a strong GFP signal (see Materials and Methods). We found that 11% of wild-type photoreceptor clusters ($n=903$) and 49% of $rbf1^{\Delta14}$ photoreceptor clusters ($n=610$) had at least one ELAV-positive cell expressing a high level of GFP–EMC, showing a four-fold increase in $rbf1^{\Delta14}$ clones (Fig. 8C). This result indicates that RBF1 is needed for correctly suppressing EMC expression in differentiating photoreceptors. This finding is also significant because it provides a molecular explanation for the synergistic effect between EMC overexpression and *rbf1* mutation. We concluded from these results that EMC expression is post-transcriptionally regulated during *Drosophila* eye development and that RBF1 plays an important role in this process.

Discussion

We report here that elevated levels of EMC, the *Drosophila* homolog of the ID family proteins, cooperate with *rbf1* mutations to interfere with *Drosophila* eye development. Analysis of this interaction led us to discover that *rbf1*-null mutant eyes exhibit intrinsic ommatidial defects, and that RBF1 is required to limit EMC expression in a cell-type-specific manner. Our study suggests that the genetic interaction between *Rb* and *Id* family genes is evolutionarily conserved, and that in *Drosophila*, Rb family proteins influence the post-transcriptional regulation of EMC protein levels.

The function of pRb tumor suppressor proteins on differentiation is one of the less understood biological

processes that pRb regulates. It is still unclear whether some of the differentiation defects associated with *pRb* deficiency are secondary consequences of deregulating cell cycle progression and/or survival. For example, a recent study demonstrated that myogenic defects caused by *pRb* deficiency could be rescued by inhibiting cell death or autophagy, indicating that the important biological process affected in this context was not differentiation (Ciavarra and Zacksenhaus, 2010). By contrast, our study strongly supports the idea that Rb family proteins do have specific functions in differentiation. Not only have we demonstrated that *rbf1* mutations in flies can lead to specific differentiation defects, but also uncovered that, like in mammals, the ID family of proteins are likely to be an important determinant of differentiation in Rb-deficient flies. Our results suggest that, similarly to their role in cell cycle progression and survival, the function of Rb family proteins in differentiation seems to be evolutionarily conserved. Perhaps, ID family proteins are targets of Rb family proteins in differentiation, similar to the way that E2F is a target in cell cycle progression and survival.

Analysis of *rbf1*-null pupal eye discs shows that RBF1 is required for proper formation of the ommatidial cluster. Although the exact molecular mechanism underlying the cone cell and photoreceptor defects is unclear, we believe that an increased amount of cellular division or cell death is probably not the cause of the phenotype. Previous studies have demonstrated that *rbf1*-null cells do not reenter the cell cycle once they start to express ELAV (Firth and Baker, 2005). In addition, we demonstrated that
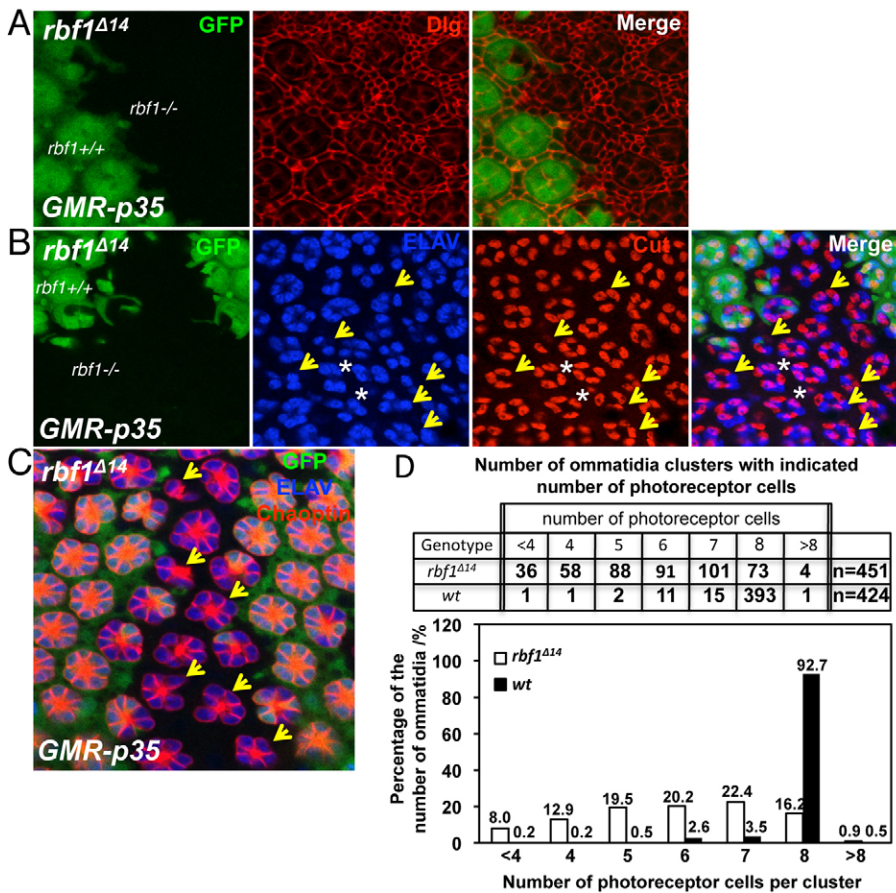
Fig. 6. The developmental defect in the *rbf1*^{Δ14} mutant ommatidia is not suppressed by blocking cell death. (**A**) Mosaic clones of *rbf1*^{Δ14} were generated as described in Fig. 5. To block cell death, baculoviral p35 proteins were expressed using GMR-p35. Pupal eye discs (42 hours APF) were immunostained with anti-ELAV (blue) and anti-Dlg (red) antibodies. Inhibition of cell death was evidenced by the extra number of interommatidial cells that were present in both wild-type and *rbf1*^{Δ14} mutant clones. (**B**) Pupal eye discs of the genotype described in A were immunostained with anti-ELAV (blue) and anti-Cut (red) antibodies. The merged image was generated by overlaying the anti-ELAV image with the anti-Cut image taken at a different focal plane in the same field of vision. Yellow arrows point out ommatidia with abnormal numbers of cone cells. Asterisks indicate ommatidia with the correct number of cone cells displaying an abnormal pattern of ELAV staining. (**C**) Pupal eye discs of the same genotype were stained with anti-ELAV (blue) and anti-Chaoptin (red) antibodies. (**D**) Control (*n*=451) and *rbf1*^{Δ14} mutant (*n*=599) ommatidia were analyzed to determine the number of photoreceptors per ommatidium. The table indicates the raw of number of ommatidial clusters with indicated number of photoreceptor cells. The bar graph shows the percentages of ommatidia, with the number of photoreceptors indicated on the *x*-axis.

Number of ommatidia clusters with indicated number of photoreceptor cells

Genotype	<4	4	5	6	7	8	>8	
rbf1^{Δ14}	36	58	88	91	101	73	4	n=451
wt	1	1	2	11	15	393	1	n=424

the inhibition of cell death does not suppress the defect. In fact, it appears to enhance the phenotype. Perhaps, *rbf1* mutant photoreceptors that fail to properly differentiate are normally eliminated by apoptosis. In this context, apoptosis serves as a quality control mechanism to ensure proper formation of ommatidia. An alternative explanation for the enhancement of the phenotype is that the surplus of surviving *rbf1* mutant cells produced by p35 expression somehow affects ommatidial integrity. Either way, we believe that the enhancement of the ommatidial defect induced by p35 expression occurs at the pupal stage because we could not detect any discernible enhancement of cell-type specification defect at the larval stage (data not shown). Although we focused our effort on analyzing *Drosophila* eye development, *rbf1* mutant flies probably possess additional developmental defects previously overlooked.

Although the phenotype observed in *rbf1* hypomorphic eyes overexpressing EMC is similar to that seen in the *rbf1*-null mutant, *rbf1*^{Δ14}, we could not directly demonstrate that the deregulated EMC activity is required for the developmental defects observed in *rbf1*-null ommatidia. To test this, we would need to generate double mutant clones of *rbf1* and *emc*. However, because *emc* itself is required for proliferation and differentiation during *Drosophila* eye development (Bhattacharya and Baker, 2009), we could not experimentally test this idea. We attempted to reduce the overall level of EMC expression in eye discs containing *rbf1*^{Δ14} clones by introducing a single copy of *d09015* or *emc*^{P5c} chromosome. However, we did not observe any appreciable changes in the ommatidial phenotype. What we do

know is that elevated expression of EMC itself is not sufficient to produce the ommatidial defect described in this study. We used a strong eye-specific Gal4 driver, GMR-Gal4, to increase the
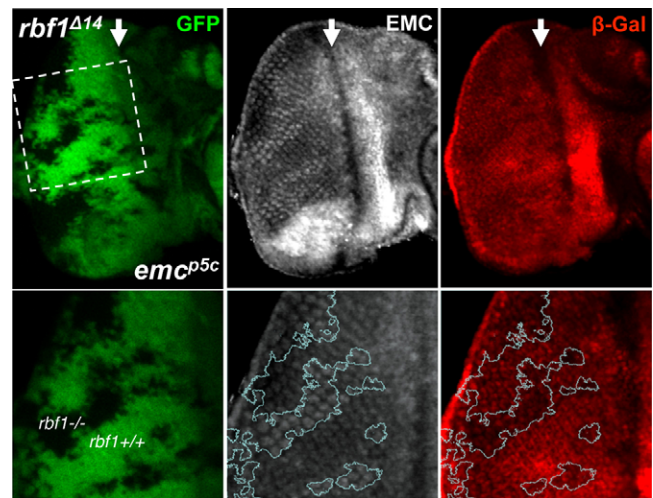

Fig. 7. RBF1 does not repress *emc* transcription. Mosaic clones of *rbf1*^{Δ14} were generated in third-instar larval eye discs that carried an *emc* enhancer trap allele, *emc*^{P5c}. β-Gal expression in the *emc*^{P5c} allele was controlled by the endogenous *emc* promoter. Immunostaining of the eye disc with anti-EMC and anti-β-Gal antibodies showed that RBF1 normally promotes the transcription of *emc* while repressing EMC protein expression. The position of the MF is marked by white arrows.
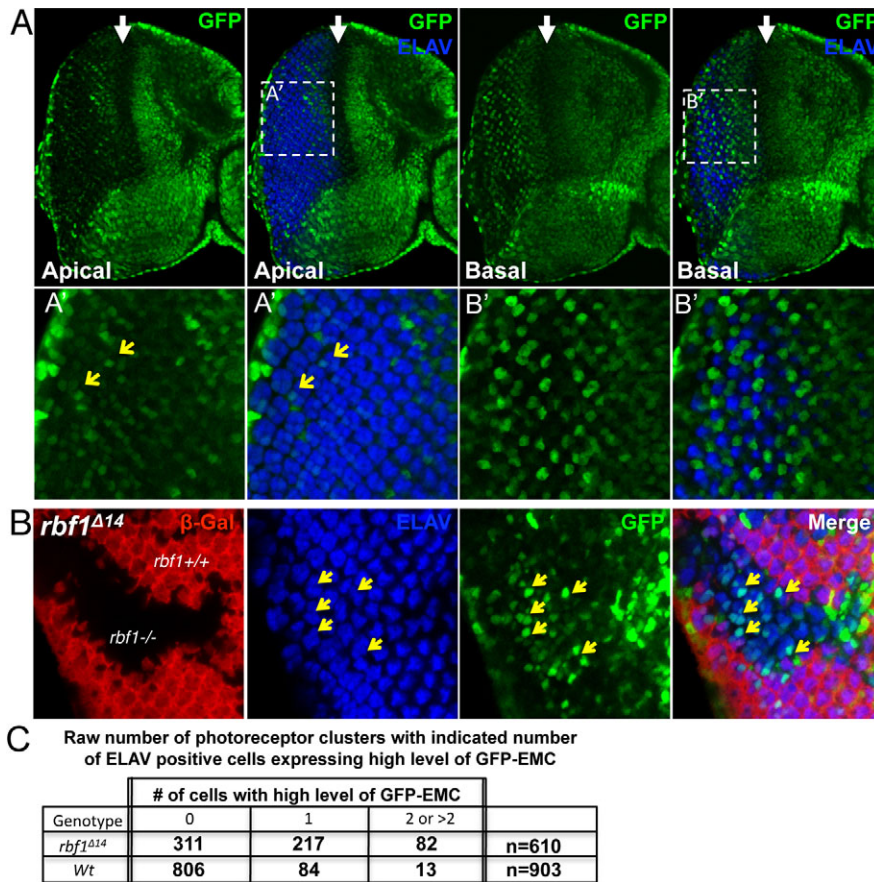
Fig. 8. Expression of ectopic EMC protein is developmentally regulated in an RBF1-dependent manner. (**A**) EMC protein tagged with GFP at the N-terminal (GFP–EMC) was expressed in the eye with the same Gal4 driver used in the genetic screen (see Materials and Methods). Third-instar eye discs were immunostained with the anti-ELAV (blue) antibody. Confocal images of a single eye disc at two different focal planes (apical and basal) are presented. The position of the MF is indicated by white arrows. Note that the GFP signal (green) is lower in the photoreceptors compared with cells anterior to the MF and between ELAV-positive cells. Few ELAV-positive cells expressed a higher level of GFP–EMC (yellow arrows). (**B**) Mosaic clones of $rbf1^{\Delta14}$ were generated in eye discs that express GFP–EMC (see Materials and Methods). Third-instar eye discs were immunostained with anti-β-Gal (red) and anti-ELAV (blue) antibodies. The $rbf1^{\Delta14}$ mutant clones are marked by the lack of β-Gal signal. An image from the apical focal plane is presented. Note that photoreceptors that express a high level of GFP–EMC can be more frequently found in the $rbf1^{\Delta14}$ clones (yellow arrows). (**C**) Table showing the number of photoreceptor clusters that contain one and two or more ELAV-positive cells that display stronger GFP signal than the neighboring ELAV-positive cells. The position of the MF is marked by white arrows.

C Raw number of photoreceptor clusters with indicated number of ELAV positive cells expressing high level of GFP-EMC

Genotype	# of cells with high level of GFP-EMC			
	0	1	2 or >2	
$rbf1^{\Delta14}$	311	217	82	n=610
Wt	806	84	13	n=903

expression level of EMC in wild-type photoreceptors, higher than what was observed in the $rbf1^{\Delta14}$ clones. However, we failed to observe any discernible eye phenotypes, indicating that factors other than EMC must participate to produce the developmental defect observed in $rbf1^{\Delta14}$ mutant clone (data not shown). Recently, Rhinoceros and the *hippo/warts* pathway have been shown to cooperate with *rbf1* mutations to control differentiation processes in the *Drosophila* eye (Nicolay et al., 2010; Steele et al., 2009). A better understanding of how these factors cooperate with *rbf1* mutations will help us to determine additional factors that contribute to the developmental defect. We are currently in the process of analyzing other alleles identified from the genetic screen, hoping to identify additional alleles that can interfere with proper ommatidial development. Nevertheless, given the similarity of the phenotypes observed between $rbf1^{120a}$ eyes overexpressing EMC and $rbf1^{\Delta14}$ eyes, EMC is likely to contribute to the developmental defect observed in $rbf1^{\Delta14}$ eyes.

One of surprising findings from our study is that the genetic interaction between *rbf1* and *emc* is not simply due to the physical interaction between their gene products. In mice, it is generally thought that ID2 is hyperactivated in *pRb* knockout mice because pRb physically binds to ID2 and limits its function. However, we found no evidence that RBF1 stably interacts with EMC. We tested this hypothesis by expressing epitope-tagged RBF1 and EMC in S2 *Drosophila* tissue culture cells and by expressing GFP-tagged EMC in *Drosophila* eyes. In the experimental conditions where transfected RBF (S2 cells) or endogenous RBF1 (in flies) co-immunoprecipitated endogenous

dE2F2, we could not detect any appreciable binding of ectopically expressed EMC proteins. We also tested physical interaction between endogenous proteins, but the result was the same (supplementary material Fig. S2). Nevertheless, two observations support the idea that the increase in EMC expression in *rbf1* mutant photoreceptors is the result of a change in the post-transcriptional regulation of EMC. First, the enhancer trap allele of *emc* revealed that RBF1 normally promotes (rather than suppresses) *emc* transcription (Fig. 5). Second, expression of the GFP–EMC construct induced by the *Act5C-Gal4* driver was also regulated by RBF1. A previous study has demonstrated that pRb proteins physically interact with Cdh1-containing APC and participate in ubiquitylation of Skp2 upon cell cycle exit (Binne et al., 2007). In another study, ID family proteins have been shown to be ubiquitylated by Cdh1-containing APC during the process of neuronal differentiation (Lasorella et al., 2006). These studies raise the interesting possibility that RBF1 might promote ubiquitylation of EMC during photoreceptor differentiation. Supporting this notion, we have discovered that EMC protein expression is also increased in *fizzy-related* (*fzr*, the *Drosophila* homolog of cdh1) mutant clones in the posterior region of the eye disc, similar to observations in $rbf1^{\Delta14}$ clones (supplementary material Fig. S4). Although this result does not directly demonstrate that RBF1 controls ubiquitylation of EMC proteins, it does show that EMC protein stability is regulated during *Drosophila* eye development by an ubiquitin-dependent mechanism. Our failure to detect any appreciable physical interaction between RBF1 and EMC could

suggest that the RBF1–Fzr–EMC protein complex might be unstable, and/or that EMC is rapidly targeted for degradation upon ubiquitylation, making it difficult to detect by the co-immunoprecipitation assay.

Previous studies have identified many transcriptional targets of pRb whose expression is deregulated in cancer cells. Often, those genes play an important role during pRb-deficient tumorigenesis. Perhaps, identification and characterization of genes whose expression is post-transcriptionally deregulated in pRb-deficient cells will further improve our understanding of the function of pRb during tumorigenesis.

Materials and Methods

Drosophila stocks
Unless otherwise specified, all fly crosses were performed at 25°C. The $rbf1$ mutants, $rbf1^{120a}$ and $rbf1^{414}$, have been previously described (Du and Dyson, 1999). UAS-EMC and emc^{P5c} were obtained from Denise Montell (Johns Hopkins School of Medicine, Baltimore, MD) (Adam and Montell, 2004) and the emc^1 allele was obtained from Bloomington Stock Center. The UAS-GFP–EMC allele was generated as follows: using complementary DNA (cDNA) generated from yw third-instar eye imaginal discs, sequences starting at the translation start site and ending at the 3′ UTR of emc were isolated by PCR and cloned into the pENTR vector (Invitrogen). The gateway system was used to transfer the emc sequence to pAGW vector (Drosophila Genomic Resource Center), which was then injected into yw embryos.

The genotype of flies containing $rbf1$ mutant clones was as follows:

$rbf1^{414}$ FRT19A/GFP^{ubi} FRT19A; eyFLP/+

$rbf1^{414}$ FRT19A GFP^{ubi} FRT19A; eyFLP/GMR-p35

$rbf1^{414}$ FRT19A/βGal^{arm} FRT19A; eyFLP/+; Act5C<CD2<Gal4, UAS-GFP–EMC/+

Genetic screen and identification of *d09015*
To sustain high levels of UAS-transgene expression in both early and late stages of *Drosophila* eye development, the following tester stocks were generated and used in the genetic screen:

yw eyFLP; Act5C<CD2<Gal4, UAS-GFP/CyO, GFP$^{act88-Gal4}$

$rbf1^{120a}$ eyFLP/FM7, GFP$^{Act88-Gal4}$; Act5C<CD2<Gal4, UAS-GFP/CyO, GFP$^{act88-Gal4}$

Males of individual XP alleles from the Exelixis *Drosophila* collection (Harvard Medical School) were crossed to virgin females of the $rbf1^{120a}$ tester stock and the adult eyes of F1 male progeny were monitored for any discernible abnormality. Selected alleles were then counter-screened against the wild-type tester stock to determine whether the abnormality was specific to $rbf1^{120a}$. $d09015$ was identified as one of the alleles that can induce an $rbf1^{120a}$-specific eye phenotype. According to the annotated information, $d09015$ contains an XP insertion on the second chromosome; however, we noticed that the insertion was present on the third chromosome. We therefore PCR-amplified the region of insertion (https://drosophila.med.harvard.edu/?q=node/32609) and sequenced it to determine whether $d09015$ had the XP insertion 72 bp upstream of the emc transcription start site.

Immunostaining and microscopy
The following antibodies were obtained from Developmental Studies Hybridoma Banks: anti-Dlg, anti-ELAV, anti-Cut, anti-Chaoptin (24B10), anti-Lz, anti-Rough and anti-β-Gal. The anti-EMC antibody was a generous gift from Yuh Nang Jan (University of California, San Francisco, CA) (Brown et al., 1995) and the anti-Senseless was from Hugo Bellen (Baylor College of Medicine, Houston, TX) (Nolo et al., 2000). The anti-C3 antibody was from Cell Signaling. For immunostaining of third-instar larval or pupal eye discs, discs were dissected and fixed with 4% paraformaldehyde for 20 minutes (30 minutes for pupal eye discs) at room temperature. Subsequently, discs were washed twice with 0.3% PBST (0.3% Triton X-100 in PBS) for 5 minutes and once with 0.1% PBST. Discs were then incubated with the primary antibody in 0.1% PBST with 5% normal goat serum at 4°C on a rotator for 16 hours. After washing five times with 0.1% PBST, discs were incubated with secondary antibody or antibodies. After washing, discs were mounted in glycerol for confocal microscopy imaging (Zeiss LSM).

Image processing of pupal eye discs
To combine pupal eye disc images at two different focal plans, confocal images at different planes were taken in the same field of vision. The channel denoting the photoreceptors from one plane and the channel denoting the cone cells at another plane were selected and merged to facilitate visualization of cone cells and photoreceptors in the same ommatidium.

Quantification
After generating $rbf1$ mutant clones and immunostaining pupal eye discs (42 hours APF) with anti-ELAV and anti-Chaoptin antibodies, confocal microscopy images were taken. Areas of the pupal eye discs that contained large clones of control and mutant photoreceptors were imaged for subsequent analysis. We selected the focal plane where wild-type ommatidia containing eight photoreceptors could be readily detected. We then counted the number of photoreceptors per ommatidium in wild-type and $rbf1^{414}$ mutant clones and determined the number of ommatidia that contained a certain number (8, 7, 6, etc) of photoreceptors in each genetic background. Mosaic ommatidia that included both wild-type and $rbf1^{414}$ mutant photoreceptors were excluded from analysis. We calculated the percentages of ommatidia (y-axis in Fig. 5C and Fig. 6D) that contained a given number of photoreceptors (x-axis in Fig. 5C and Fig. 6D).

To count ommatidia that contained one or more ELAV-positive cells expressing high levels of GFP–EMC, confocal images of the apical plane of numerous imaginal discs were taken. The boundaries of the photoreceptor clusters were determined by ELAV staining. If a cluster contained a distinct nuclear GFP signal that was distinguishably stronger than the neighboring cells within and outside the cluster, it was scored as an ommatidium that contained a photoreceptor expressing a high level of GFP–EMC.

References
Adam, J. C. and Montell, D. J. (2004). A role for *extra macrochaetae* downstream of Notch in follicle cell differentiation. *Development* **131**, 5971-5980.

Bhattacharya, A. and Baker, N. E. (2009). The HLH protein Extramacrochaetae is required for R7 cell and cone cell fates in the Drosophila eye. *Dev. Biol.* **327**, 288-300.

Binne, U. K., Classon, M. K., Dick, F. A., Wei, W., Rape, M., Kaelin, W. G., Jr, Naar, A. M. and Dyson, N. J. (2007). Retinoblastoma protein and anaphase-promoting complex physically interact and functionally cooperate during cell-cycle exit. *Nat. Cell Biol.* **9**, 225-232.

Brown, N. L., Sattler, C. A., Paddock, S. W. and Carroll, S. B. (1995). Hairy and emc negatively regulate morphogenetic furrow progression in the Drosophila eye. *Cell* **80**, 879-887.

Calo, E., Quintero-Estades, J. A., Danielian, P. S., Nedelcu, S., Berman, S. D. and Lees, J. A. (2010). Rb regulates fate choice and lineage commitment in vivo. *Nature* **466**, 1110-1114.

Ciavarra, G. and Zacksenhaus, E. (2010). Rescue of myogenic defects in Rb-deficient cells by inhibition of autophagy or by hypoxia-induced glycolytic shift. *J. Cell Biol.* **191**, 291-301.

Dimova, D. K., Stevaux, O., Frolov, M. V. and Dyson, N. J. (2003). Cell cycle-dependent and cell cycle-independent control of transcription by the Drosophila E2F/RB pathway. *Genes Dev.* **17**, 2308-2320.

Du, W. and Dyson, N. (1999). The role of RBF in the introduction of G1 regulation during Drosophila embryogenesis. *EMBO J.* **18**, 916-925.

Dyson, N. (1998). The regulation of E2F by pRB-family proteins. *Genes Dev.* **12**, 2245-2262.

Firth, L. C. and Baker, N. E. (2005). Extracellular signals responsible for spatially regulated proliferation in the differentiating Drosophila eye. *Dev. Cell* **8**, 541-551.

Gu, W., Schneider, J. W., Condorelli, G., Kaushal, S., Mahdavi, V. and Nadal-Ginard, B. (1993). Interaction of myogenic factors and the retinoblastoma protein mediates muscle cell commitment and differentiation. *Cell* **72**, 309-324.

Iavarone, A., Garg, P., Lasorella, A., Hsu, J. and Israel, M. A. (1994). The helix-loop-helix protein Id-2 enhances cell proliferation and binds to the retinoblastoma protein. *Genes Dev.* **8**, 1270-1284.

Iavarone, A., King, E. R., Dai, X. M., Leone, G., Stanley, E. R. and Lasorella, A. (2004). Retinoblastoma promotes definitive erythropoiesis by repressing Id2 in fetal liver macrophages. *Nature* **432**, 1040-1045.

Ji, P., Jiang, H., Rekhtman, K., Bloom, J., Ichetovkin, M., Pagano, M. and Zhu, L. (2004). An Rb-Skp2-p27 pathway mediates acute cell cycle inhibition by Rb and is retained in a partial-penetrance Rb mutant. *Mol. Cell* **16**, 47-58.

Lasorella, A., Iavarone, A. and Israel, M. A. (1996). Id2 specifically alters regulation of the cell cycle by tumor suppressor proteins. *Mol. Cell. Biol.* **16**, 2570-2578.

Lasorella, A., Noseda, M., Beyna, M., Yokota, Y. and Iavarone, A. (2000). Id2 is a retinoblastoma protein target and mediates signalling by Myc oncoproteins. *Nature* **407**, 592-598.

Lasorella, A., Uo, T. and Iavarone, A. (2001). Id proteins at the cross-road of development and cancer. *Oncogene* **20**, 8326-8333.

Lasorella, A., Rothschild, G., Yokota, Y., Russell, R. G. and Iavarone, A. (2005). Id2 mediates tumor initiation, proliferation, and angiogenesis in Rb mutant mice. *Mol. Cell. Biol.* **25**, 3563-3574.

Lasorella, A., Stegmuller, J., Guardavaccaro, D., Liu, G., Carro, M. S., Rothschild, G., de la Torre-Ubieta, L., Pagano, M., Bonni, A. and Iavarone, A. (2006). Degradation of Id2 by the anaphase-promoting complex couples cell cycle exit and axonal growth. *Nature* **442**, 471-474.

Lipinski, M. M. and Jacks, T. (1999). The retinoblastoma gene family in differentiation and development. *Oncogene* **18**, 7873-7882.

Moon, N. S., Di Stefano, L. and Dyson, N. (2006). A gradient of epidermal growth factor receptor signaling determines the sensitivity of rbf1 mutant cells to E2F-dependent apoptosis. *Mol. Cell. Biol.* **26**, 7601-7615.

Nicolay, B. N., Bayarmagnai, B., Moon, N. S., Benevolenskaya, E. V. and Frolov, M. V. (2010). Combined inactivation of pRB and hippo pathways induces dedifferentiation in the Drosophila retina. *PLoS Genet.* **6**, e1000918.

Nolo, R., Abbott, L. A. and Bellen, H. J. (2000). Senseless, a Zn finger transcription factor, is necessary and sufficient for sensory organ development in Drosophila. *Cell* **102**, 349-362.

Reinke, R., Krantz, D. E., Yen, D. and Zipursky, S. L. (1988). Chaoptin, a cell surface glycoprotein required for Drosophila photoreceptor cell morphogenesis, contains a repeat motif found in yeast and human. *Cell* **52**, 291-301.

Sherr, C. J. (1996). Cancer cell cycles. *Science* **274**, 1672-1677.

Steele, L., Sukhanova, M. J., Xu, J., Gordon, G. M., Huang, Y., Yu, L. and Du, W. (2009). Retinoblastoma family protein promotes normal R8-photoreceptor differentiation in the absence of rhinoceros by inhibiting dE2F1 activity. *Dev. Biol.* **335**, 228-236.

Stevaux, O., Dimova, D. K., Ji, J. Y., Moon, N. S., Frolov, M. V. and Dyson, N. J. (2005). Retinoblastoma family 2 is required in vivo for the tissue-specific repression of dE2F2 target genes. *Cell Cycle* **4**, 1272-1280.

Thibault, S. T., Singer, M. A., Miyazaki, W. Y., Milash, B., Dompe, N. A., Singh, C. M., Buchholz, R., Demsky, M., Fawcett, R., Francis-Lang, H. L. et al. (2004). A complementary transposon tool kit for Drosophila melanogaster using P and piggyBac. *Nat. Genet.* **36**, 283-287.

Thomas, D. M., Carty, S. A., Piscopo, D. M., Lee, J. S., Wang, W. F., Forrester, W. C. and Hinds, P. W. (2001). The retinoblastoma protein acts as a transcriptional coactivator required for osteogenic differentiation. *Mol. Cell* **8**, 303-316.

van den Heuvel, S. and Dyson, N. J. (2008). Conserved functions of the pRB and E2F families. *Nat. Rev. Mol. Cell Biol.* **9**, 713-724.

Wang, H., Bauzon, F., Ji, P., Xu, X., Sun, D., Locker, J., Sellers, R. S., Nakayama, K., Nakayama, K. I., Cobrinik, D. et al. (2010). Skp2 is required for survival of aberrantly proliferating Rb1-deficient cells and for tumorigenesis in Rb1+/− mice. *Nat. Genet.* **42**, 83-88.